# Solvatochromic Shift of Brooker's Merocyanine: Hartree–Fock Exchange in Time Dependent Density Functional Calculation and Hydrogen Bonding Effect

Takuya Wada,[†] Hiroshi Nakano,*[,†,‡] and Hirofumi Sato*[,†,‡]

[†]Department of Molecular Engineering, Kyoto University, Kyoto Daigaku Katsura, Kyoto 615-8510, Japan
[‡]Elements Strategy Initiative for Catalysts and Batteries, Kyoto University, Kyoto 615-8245, Japan

S *Supporting Information*

ABSTRACT: The Brooker's merocyanine exhibits a large hypsochromic shift from an apolar aprotic solvent to a polar protic solvent. Quantum chemical calculations have been performed to study the solvatochromism, but there remained a discrepancy between the calculated and experimental solvatochromic shifts. In this paper we evaluate quantum mechanically the excitation energies of the Brooker's merocyanine in water, methanol, acetonitrile, and dichloromethane to investigate what are important factors to accurately model the solvatochromism of the dye by using TDDFT in combination with implicit and explicit solvation models including the PCM, PCMSMD, RISM-SCF-SEDD, and mean-field QM/MM. The results severely depend on the density functional, especially on the amount of Hartree–Fock exchange included in the functional. Furthermore, an explicit description of the solute–solvent hydrogen bonds makes a non-negligible contribution to the shift. The experimental large solvatochromic shift can be accurately reproduced by the TDDFT/RISM-SCF-SEDD and mean-field QM/MM calculations with the LC-BOP functional, although the excitation energies in solutions are considerably overestimated. We also estimated the excitation energies and the solvatochromic shift at the SAC-CI/RISM-SCF-SEDD and mean-field QM/MM level, which are in very good agreement with the experimental values. These results indicate that if an explicit solvent model is used, TDDFT calculations using such a long-range corrected functional can accurately model the solvatochromism. However, an *ab initio* quantum chemical method including sufficient electron correlation effects is required to reproduce not only the solvatochromism but also the excitation energies in solutions.

solvatochromic shifts of Brooker's merocyanine

SDFs of water molecules
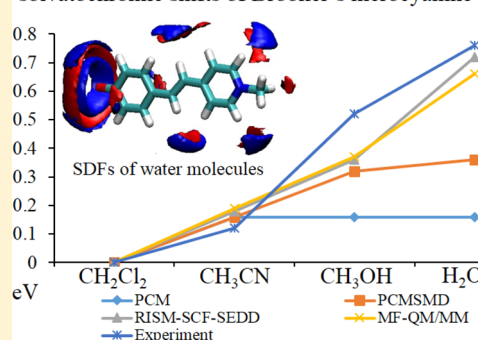
INTRODUCTION

It is well-known that the excitation energy of a certain class of molecules can significantly and sensitively depend on the environment, for example, the solvent of its solution, the interior or surface of a vesicle, protein, and membrane to which such a molecule binds.[1–8] These molecules have therefore been utilized as molecular probes to investigate both the macroscopic and microscopic characters of the surrounding media; polarity, ability to act as a hydrogen bonding donor or acceptor, etc. This leads to a concept of "polarity scale" with which we can estimate the polarity of the environment around a dye molecule and the interactions between them. There are some solvent polarity scales, for example, those of Reichardt $E_T(30)$, Z scale of Kosower, and π^* scale of Kamlet.[1,2] The Brooker's merocyanine is one of such dye molecules, which has been studied for a long time both experimentally and theoretically.[9–25] It exhibits a large hypsochromic shift from less polar aprotic to more polar protic solvents. For example, it shows a 0.76 eV blue shift from dichloromethane to water.[23] The observed absorption is attributed to the $S_0–S_1$ $\pi–\pi^*$ excitation with some intramolecular charge transfer (CT) character.[24] The large hypsochromic shift has been explained by

considering two resonance structures of benzenoid and quinoid forms as shown in Figure 1.[9,10,15,16,23] The ground and first excited states can be characterized as mixed states of the two resonance forms with different weights. The excitation energy changes when the weight of each resonance form varies in the ground and excited state. Since the benzenoid form is much
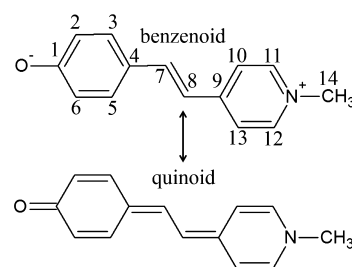

Figure 1. Brooker's merocyanine represented by the two resonance forms. The carbon atoms are indexed to present bond lengths (Table 4).

more polar than the quinoid form, it becomes dominant in polar solvents. Moreover, since the phenolate oxygen can form hydrogen bonds with protic solvent molecules,[12,16,23,24] the weight of the benzenoid form further increases in the ground state. This results in further stabilization of the ground state as compared to the excited state with quinoid character and increases the excitation energy. Thus, the Brooker's merocyanine is a good indicator to measure the polarity and hydrogen bond donor ability of the solvent. Furthermore, it has many points in common with the Reichardt dye, whose excitation has intramolecular CT character and can form hydrogen bonds between the phenolate oxygen and hydrogens of protic solvents.[1,2,26] Therefore, detailed understanding of the optical absorption of Brooker's merocyanine in various solvents is valuable for understanding the character of not only the dye itself but also other dye molecules exhibiting a similar solvatochromism.

In order to study theoretically the solvatochromism of Brooker's merocyanine, a quantum mechanical method is necessary to evaluate the excitation energy while taking into account the solvation effects. There have been many such theoretical studies using semiempirical or time-dependent density functional theory (TDDFT) in combination with implicit or explicit solvation models.[15,16,18−20,24,25] Botrel et al. performed Complete Neglect of Differential Overlap/Spectroscopic parametrization Configuration Interaction (CNDO/SCI) calculation with image charge method, where the solvation effects were taken into account implicitly. They optimized the geometries of Brooker's merocyanine and observed that the structure changes from quinoid to benzenoid forms by increasing the dielectric constant in their solvation model. The calculated solvatochromic shift by about 1 eV is in good agreement with experimental value from trichloromethane to water (0.81 eV), but the excitation energies themselves were overestimated by as much as 1 eV.[15] Luzhkov and Warshel have performed their semiempirical quantum mechanical extension of the consistent force field (QCFF)/SOL calculation. The Langevin dipole model was employed to mimic the microscopic solvation effects, and the solvatochromic shift was reproduced semiquantitatively.[25] Morley et al. have studied in detail the mechanism of the solvatochromism both experimentally and theoretically. Their ^{1}H and ^{13}C NMR experiments suggest that the resonance hybrid of the Brooker's merocyanine in the ground state is weighted toward the benzenoid form even in an aprotic solvent with a relatively low dielectric constant. They also showed that the large hypsochromic shift observed arises from both a dielectric effect and hydrogen bonding effects. They optimized the geometry by AM1/COSMO (conductor-like screening model) and PM3/COSMO calculations followed by the multielectron configuration interaction treatment to evaluate the excitation energies in solutions. The hypsochromic shift from apolar solvent to polar solvent has been partly reproduced, but the extent of the shift is underestimated because of the neglect of the explicit hydrogen bonding effects.[16] Adjaye-Mensah et al. employed TDDFT/PCMSMD (polarizable continuum model solvation model density) with the B3LYP and CAM-B3LYP functionals to evaluate the solvatochromism of a benzo-fused analogue of Brooker's merocyanine. The calculated solvatochromic shifts in the absorption from acetone to water were 0.12 and 0.34 eV with B3LYP and CAM-B3LYP functionals, respectively, which were considerably underestimated with respect to their experimental value of 0.80 eV.[18] Murugan et al. conducted

quantum mechanics/molecular mechanics (QM/MM) Car−Parrinello molecular dynamics calculations at the DFT(BLYP) level with a plane wave basis. They used a polarizable force field for water and trichloromethane to investigate the solvent back polarization effects on the excitation of Brooker's merocyanine. They calculated the excitation energies in the solvents at the CAM-B3LYP/TZVP level including also the nonequilibrium solvation effects based on the response theory at 80 configurations taken from the trajectory. The solute−solvent hydrogen bonding effects were thus taken into account in their calculations. They showed that solvent back polarization effects are not so important. They also investigated the solute−solvent CT effects by including some water molecules in the QM region and found that it is less important. The average excitation energies were 2.92 and 2.56 eV for water and trichloromethane, respectively, and the solvatochromic shift was 0.36 eV. The value for water solution was in good agreement with the experimental value of 2.81 eV. On the other hand, the value for trichloromethane solution was considerably overestimated, and then the solvatochromic shift was underestimated against the experimental values of 2.00 and 0.81 eV, respectively. They suggested that the disagreement for trichloromethane solution is possibly due to the neglect of the solute−solvent dispersion interactions in their excitation energy calculations, but it has not been verified.

Based on these studies, many important features about the solvatochromism of Brooker's merocyanine have been elucidated. However, there remains a challenge to reveal the reason why one of the most elaborate calculations by Murugan et al. using TDDFT with an explicit solvation model considerably underestimates the experimentally observed large solvatochromic shift (note that most of the calculations using implicit solvation models also underestimate it). It is valuable to address this problem because TDDFT has been and will be extensively utilized to study the solvatochromism of various molecules for which quantitative estimations are required.[27−37] Note that TDDFT currently has an inherent problem that the result substantially depends on the functional and should be carefully examined.[38−45] It implies not only the excitation energies of Brooker's merocyanine in solutions but also its solvatochromic shift severely depends on the functional.

The aim of the present study is thus to clarify what is important to accurately reproduce a large solvatochromic shift of the merocyanine dye in protic and aprotic solvents. To calculate excitation energies, we used TDDFT with various functionals to investigate the functional dependence of the solvatochromic shifts and especially focus on the importance of Hartree−Fock (HF) exchange included in the functionals.[46] To take into account the solvation effects and estimate the importance of microscopic description of solvation, we employed the PCM (without solute−solvent nonelectrostatic interactions) and the PCMSMD as implicit solvation models[47−51] and the reference interaction site model-self-consistent field-spatial electron density distribution (RISM-SCF-SEDD)[52−58] and mean-field QM/MM (MF-QM/MM) methods[59−61] as explicit solvation models, respectively. These explicit solvation models can describe the solute−solvent hydrogen bonding effects as in the QM/MM calculations[62−65] while saving much of the computational costs as compared to QM/MM molecular dynamics calculations because of the mean-field approximation employed in the models. The present results show that for quantitative evaluation of large solvatochromic shifts of the dye, it is

Table 1. Excitation Energies and Solvatochromic Shifts (in Parentheses) from Dichloromethane at the TDDFT/6-31+G(d,p)/PCMSMD Level[a]

functional		water	methanol	acetonitrile	dichloromethane
SVWN		2.38(−0.04)	2.39(−0.03)	2.40(−0.02)	2.42(0.00)
BLYP		2.36(−0.04)	2.37(−0.03)	2.38(−0.02)	2.40(0.00)
PBE		2.38(−0.03)	2.40(−0.01)	2.40(−0.01)	2.41(0.00)
BP86		2.38(−0.04)	2.39(−0.03)	2.41(−0.01)	2.42(0.00)
BOP		2.37(−0.03)	2.37(−0.03)	2.39(−0.01)	2.40(0.00)
TPSS		2.43(−0.03)	2.43(−0.03)	2.45(−0.01)	2.46(0.00)
TPSSh	[10%]	2.52(0.01)	2.52(0.01)	2.52(0.01)	2.51(0.00)
B3LYP	[20%]	2.56(0.05)	2.56(0.05)	2.53(0.02)	2.51(0.00)
B3PW91	[20%]	2.58(0.05)	2.57(0.05)	2.55(0.02)	2.53(0.00)
PBE0	[25%]	2.63(0.08)	2.62(0.07)	2.58(0.03)	2.55(0.00)
M06	[27%]	2.59(0.08)	2.58(0.07)	2.54(0.03)	2.51(0.00)
BH&HLYP	[50%]	2.89(0.23)	2.86(0.20)	2.76(0.10)	2.66(0.00)
M06-2X	[54%]	2.78(0.23)	2.75(0.20)	2.64(0.09)	2.55(0.00)
M06-HF	[100%]	3.09(0.52)	3.04(0.47)	2.79(0.22)	2.57(0.00)
CAM-B3LYP		2.82(0.23)	2.80(0.21)	2.69(0.10)	2.59(0.00)
LC-BOP		2.94(0.36)	2.90(0.32)	2.74(0.16)	2.58(0.00)
LC-BLYP		2.93(0.35)	2.89(0.31)	2.73(0.15)	2.58(0.00)
LC-BVWN		2.95(0.37)	2.90(0.32)	2.74(0.16)	2.58(0.00)
LC-BPBE		2.96(0.36)	2.92(0.32)	2.76(0.16)	2.60(0.00)
TDHF		3.38(0.41)	3.34(0.37)	3.16(0.19)	2.97(0.00)
expt		2.81(0.76)	2.57(0.52)	2.17(0.12)	2.05(0.00)

[a]Calculations were performed at the geometries optimized at the LC-BOP/6-31+G(d,p)/PCMSMD level in solutions. LDA, GGA, meta-GGA, Hybrid, and LC Functionals are listed from top to bottom. The hybrid functionals are sorted in the order of increasing amount of HF exchange included (written in brackets). Units are in eV.

essential both to choose a functional which properly treats HF exchange in the (TD)DFT calculations and to take into account the microscopic description of the solvation. We also show that the accurate evaluation of the absolute values of excitation energy of the dye in solutions further requires a quantum chemical method with adequate electron correlation effects such as the symmetry adapted cluster/configuration interaction (SAC-CI) method.[66,67]

METHODS

The solvent effects were treated by both of the implicit and explicit solvent models. The PCM and PCMSMD were employed as the implicit solvent models. The former was used without including nonelectrostatic solute−solvent interactions, but the latter takes into account also such interactions as CDS (cavitation, dispersion, local solvent structure changes) corrections. Note that the solute−solvent specific interactions like hydrogen bonds are also implicitly taken into account in the parametrization of the cavity radii and especially the CDS terms in the PCMSMD model.[49] In the excitation energy calculations, nonequilibrium solvation effects were included to model the solvent electronic polarization associated with the vertical excitation of the solute.[68−70]

We performed the RISM-SCF-SEDD and MF-QM/MM calculations to explicitly model the solvent effects. In the former method, the ensemble of solvent configurations is represented by radial distribution functions (RDFs) between the solute and solvent atoms. The RDFs are determined by the reference interaction site model (RISM) theory which consists of the site−site Ornstein−Zernike equation and a closure relation. The Kovalenko-Hirata closure was used in this study.[53] The spatial electron density distribution (SEDD) of the solute molecule is fitted with auxiliary basis sets (ABSs) attached to solute atoms so as to reproduce the solute electrostatic

potential.[57] The Fock operator includes the electrostatic interactions between the solute electrons and the solvent charge distribution represented by RDFs as follows

$$F_{\mu\nu}^{solv} = F_{\mu\nu}^{gas} - \sum_{i}^{N_{ABS}} \langle \chi_\mu | \hat{d}_i | \chi_\nu \rangle \cdot n^V \sum_\gamma^{solv} q_\gamma$$

$$\times \iint \frac{f_i(|\mathbf{r}' - \mathbf{r}_\alpha|)}{|\mathbf{r} - \mathbf{r}'|} \{g_{\alpha\gamma}(|\mathbf{r} - \mathbf{r}_\alpha|) - 1\} d\mathbf{r} d\mathbf{r}' \quad (1)$$

where $F_{\mu\nu}^{gas}$ is the Fock operator in the gas phase, $\hat{d}_i$ is the population operator of the i-th ABS $f_i(\mathbf{r})$, N_{ABS} is the number of the ABSs, n^V and q_γ are the number density and partial charge of the γ site of the solvent molecules, respectively, and $g_{\alpha\gamma}(r)$ is the RDF between the solute α site and the solvent γ site. The electronic state of the solute molecule is thus polarized by solvation effects. Since the solute wave function and the solvent distribution depend on each other, they are calculated iteratively and self-consistently. This method has been shown to give quantitative results for many systems in both aprotic and protic solvents due to the explicit description of solvent molecules.[52] Note also that the RISM-SCF method (using not the SEDD treatment shown above but the point charge description for solute electron density) has recently been applied to a merocyanine dye with conjugated chains (steptopolymethinemerocyanine) to clarify the excitation energy dependence on its chain length in water, methanol, and acetonitrile.[71] The MF-QM/MM method is similar to the RISM-SCF-SEDD method in that the solute wave function is determined under the mean electrostatic potentials generated by an ensemble of solvent configurations (the mean-field approximation). In the MF-QM/MM method, however, the solvent distribution is sampled from MD calculations. The Fock operator becomes

$$F_{\mu\nu}^{solv} = F_{\mu\nu}^{gas} - \left\langle \chi_\mu \left| \left\langle \sum_m^{MM} \frac{q_m}{|\mathbf{r} - \mathbf{r}_m|} \right\rangle \right| \chi_\nu \right\rangle$$
(2)

where q_m and $\mathbf{r}_m$ are the partial charge and the position of the m-th solvent atom, respectively. The $\langle \cdots \rangle$ denotes an ensemble average of the quantity. The long-range electrostatic interactions were taken into account as in the QM/MM-Ewald method of Nam et al.[61,72] This method is quite accurate and robust because the electron distribution of the solute molecule is handled essentially without approximation. As in the RISM-SCF-SEDD method, since the solute wave function and the solvent distribution depend on each other, QM calculations (under the mean electrostatic potentials of solvent) and MD samplings are performed iteratively to achieve the self-consistency. It should be stressed that the solute charge distribution used in the MD samplings is calculated with the polarized wave function (or molecular orbitals) obtained by solving the Schrödinger (Kohn–Sham) equation in which the Fock operator is expressed as eq 2. It means that the solute polarization effects are effectively included in the MD calculations. Since this method is rigorously formulated based on the variational principle for QM/MM free energy,[59] it has been shown to give a solvation structure and a free energy profile of a solute molecule in solution in excellent agreement with those from a QM/MM-MD calculation.[60,61] It should also be noted that the MF-QM/MM method is similar to other QM/MM-based methods in which the solute electronic state is determined under an ensemble of configurations of solvent molecules.[73−78] These methods have been successfully applied to many chemical applications including excited state calculations in solution.

COMPUTATIONAL DETAILS

The geometries of the merocyanine dye in solutions were optimized at the LC-BOP/6-31+G(d,p) level. We considered only the trans isomer according to experimental observations.[11,12,16] The vertical excitation energies were calculated using TDDFT with various functionals listed in Table 1.[79−101] The 6-31+G(d,p) basis set was employed. We also tested the aug-cc-pVTZ basis set to evaluate the excitation energies in solutions and found that the variations in the excitation energy were no more than 0.1 eV.

In the RISM-SCF-SEDD and MF-QM/MM calculations, the LJ parameters of all atoms in the system and partial charges of solvent atoms are necessary. Those values were taken from the literature[102−106] and listed in the Supporting Information. The number density of solvent atoms used in the RISM-SCF-SEDD calculations were 0.0333 Å^{-3} for water, 0.0148 Å^{-3} for methanol, 0.0114 Å^{-3} for acetonitrile, and 0.00934 Å^{-3} for dichloromethane, respectively. The other specific parameters necessary for the RISM-SCF-SEDD calculations were the grid spacing (0.025 Bohr) and the number of grid points (4,096 points). The s-type orbitals in the 6-31+G(d,p) basis were taken as the auxiliary basis set to represent the spatial electron density distribution (SEDD) of the solute molecule.[57] In the MF-QM/MM calculations, the systems were composed of one solute molecule (Brooker's merocyanine) and 860 solvent molecules. The periodic boundary condition was employed, and the long-range electrostatic interactions were treated by the Ewald summation. The box sizes of the systems were determined initially by the NPT calculations. The equilibrium solvent configurations were then sampled from NVT

calculations. The mean electrostatic potentials of solvent were generated using 500 configurations taken from 1.5 ns production run after 100 ps equilibration. We checked the dependence of the excitation energy on the number of configurations (see the Supporting Information) and found that more than 100 configurations were sufficient to obtain the converged result as has been shown by Canuto and co-workers.[73] The temperature was 298.15 K in all of the systems. For other technical details of the RISM-SCF-SEDD and MF-QM/MM methods, please refer to the original articles.[57,61] Since nonpolarizable force fields were used in these models, electronic polarization of solvent associated with the vertical excitation of the solute were not explicitly taken into account. To partially correct this deficiency, we decided to include the above-mentioned nonequilibrium solvation effects evaluated by using the PCM model into the excitation energies calculated by these explicit solvation models. These effects were estimated by performing TDDFT/PCM excitation energy calculations with fixed apparent surface charges determined in the ground state and subtracting these values from the TDDFT/PCM excitation energies including the nonequilibrium solvation effects. The values were about −0.2 eV in all of the calculations of solutions in the present study. Note that it has been shown by Murugan et al.[19] in their excitation energy calculations that the effects of the solvent polarization effects due to the electrostatic interactions with the solute molecule at the ground state and of the solute−solvent CT interactions are relatively small. Therefore, it is expected that the solvent models used in the present work (empirical nonpolarizable models) can give reasonable results.

The QM and MD calculations were performed by modified versions of the GAMESS[107] and DL_POLY 2.20 packages,[108] respectively, unless otherwise noted.

RESULTS AND DISCUSSION

Functional Dependence of the Solvatochromic Shift. We first investigate the functional dependence of the solvatochromic shift of the S_0-S_1 excitation energy in solutions by using the PCMSMD. The excitation energies and the resulting solvatochromic shifts calculated with various functionals are compiled in Table 1. The functionals can be categorized as local density approximation (LDA), generalized gradient approximation (GGA), meta generalized gradient approximation (meta-GGA), hybrid, and long-range corrected (LC) functionals. The results show some clear tendencies: First, the LDA, GGA, and meta-GGA functionals, which do not include any HF exchange, give wrong solvatochromic shifts (red shift).[109] The red shift from dichloromethane to water is from 0.03 to 0.05 eV, and the gradient and higher corrections to exchange correlation (XC) functional hardly affects the extent of the shift. The absolute values of the excitation energy are also similar to each other. Second, the hybrid functionals predict the correct solvatochromic shift (blue shift), and the amount of HF exchange in the hybrid functionals has significant impact on and correlate well with the extent of the shift. The functionals with a small amount of HF exchange such as TPSSh (10%), B3LYP, and B3PW91 (20%) give a small solvatochromic shift from dichloromethane to water by 0.01, 0.05, and 0.05 eV, respectively. On the other hand, the functionals with more than or equal to 50% amount of HF exchange such as BH&HLYP (50%), M06-2X (54%), and M06-HF (100%) give 0.23, 0.23, and 0.52 eV shifts, respectively. Third, the LC functionals give solvatochromic shifts whose extent are among

those calculated by using hybrid functionals with more than 50% HF exchange. All of the LC functionals give a 0.36 eV solvatochromic shift[110] except for the CAM-B3LYP functional which gives a 0.24 eV shift. It should be noted that while the CAM-B3LYP functional includes only 65% HF exchange in the long-range limit, the other LC functionals asymptotically recover 100% HF exchange. These results clearly demonstrate the importance of HF exchange included in the XC functionals to correctly model the solvatochromism of the merocyanine dye in different environment. This can be also verified from the shift by 0.41 eV obtained from a time dependent Hartree–Fock (TDHF) calculation, though it considerably overestimates the excitation energies with respect to the experimental values most probably because of the neglect of electron correlation.

In order to investigate the reason why HF exchange considerably affects the solvatochromic shift, we examined the dipole moment of the solvated merocyanine dye in the ground and excited states calculated at the SVWN, BLYP, B3LYP, and LC-BOP levels, which are listed in Table 2. It can be observed

Table 2. Dipole Moments (in Debye) in the Ground/Excited States Calculated at the (TD)DFT/6-31+G(d,p)/PCMSMD Level

solvent	SVWN	BLYP	B3LYP	LC-BOP
water	33.8/25.0	33.7/24.6	35.5/23.9	38.6/23.3
methanol	33.1/24.9	33.0/24.5	34.7/23.9	37.9/23.0
acetonitrile	30.2/23.7	30.1/23.4	31.6/23.2	34.6/21.7
dichloromethane	27.9/23.5	27.7/23.3	28.9/23.5	31.6/22.2

that as an XC functional includes a larger amount of HF exchange, the dye in the ground state (excited state) has a larger (smaller) dipole moment; in other words, it has more benzenoid (quinoid) character. This can be understood from the fact that a DFT calculation using a functional with no or a small amount of HF exchange tends to make the electron distribution more delocalized in the ground state due to the self-interaction.[40,43] Since a larger amount of HF exchange therefore makes more significant the difference between the electronic distributions of and then the solvation effects on the ground and the excited states of the dye, the solvatochromic shift becomes large when using such functionals.

The degree of charge localization (or the weight of the benzenoid form) in the ground state can be estimated from the partial charges on atoms or fragments of the dye. The fragments considered here are the phenolate and methylpyridinium ones, both of which do not include the carbon and hydrogen atoms in the bridge part of the dye (C7 and C8 carbon atoms in Figure 1). They were evaluated from the natural population analysis[111,112] and listed in Table 3. For all of the functionals, the absolute values of charges on the fragments become larger in polar solvents than in apolar solvents and especially in protic solvents than in aprotic solvents. This indicates that the benzenoid form becomes more

dominant than the quinoid form in a more polar protic solvent. It can also be observed that the absolute values of the fragment charges increase as the functional includes a larger amount of HF exchange. The fragment charges are very similar to each other when the SVWN and the BLYP functional are used, both of which do not include HF exchange.

We also calculated the bond lengths of the dye to check the functional influence on the geometry in solutions because the above results indicate that the weight of each resonance structure (benzenoid or quinoid form) in the ground state can vary considerably when using different functionals and then have impact on the solvatochromic shift. The representative bond lengths are given in Table 4 calculated at the DFT/PCMSMD/6-31+G(d,p) with B3LYP and LC-BOP functionals. The experimental bond lengths in a trihydrate crystal were also presented.[113] Both of the theoretical results show that the weight of the benzenoid form becomes larger as the solute interacts electrostatically more strongly with protic solvent with higher dielectric constant. The B3LYP functional tends to give a slightly more quinoid-like structure. The largest change is observed in the C7–C8 bond in the bridge part of the dye. The geometry optimized using the LC-BOP functional is in better agreement with that in a trihydrate crystal than that using the B3LYP functional. When we use the structures optimized at the B3LYP/PCMSMD level and then perform TDDFT calculations with the B3LYP and LC-BOP functionals, the obtained solvatochromic shifts from dichloromethane to water are 0.06 and 0.25 eV, respectively. The latter value is smaller by 0.11 eV than that obtained at the structures optimized using the LC-BOP functional (0.36 eV). This result indicates that though the extent is seemingly small, the functional dependence of the geometry cannot be negligible, and the solvatochromic shift can be considerably underestimated when we use a functional with a small amount of HF exchange for geometry optimization.

It has been shown that the range separation parameter (μ) in an LC functional can have a significant impact on the excitation energies in TDDFT calculations.[46,114] Thus, we calculated the excitation energies and solvatochromic shifts by varying μ in the LC-BOP functional at the geometries optimized with $\mu = 0.33$ bohr^{-1} (Figure 2).[115,116] When μ is zero, the LC-BOP functional reverts to the original BOP functional with no HF exchange. On the other hand, when μ is large enough, 100% HF exchange works throughout all the distances between two electrons. As we have seen that increasing the amount of HF exchange increases the excitation energies and solvatochromic shift, expanding the range where HF exchange works by using a large value of μ also considerably increases those values. μ greater than 1.0 bohr^{-1} gives a slightly larger solvatochromic shift of about 0.43 eV, which is almost equal to the solvatochromic shift of 0.41 eV evaluated by TDHF, than the 0.36 eV shift for μ of the default value (0.33 bohr^{-1}). However, it considerably overestimates the excitation energies with respect to the experimental values.

Table 3. Phenolate/Methylpyridinium Fragment Charges in Solutions in the Ground State Calculated from Natural Population Analysis at the DFT/6-31+G(d,p)/PCMSMD Level

solvent	SVWN	BLYP	B3LYP	LC-BOP
water	−0.69/0.66	−0.70/0.66	−0.75/0.70	−0.83/0.78
methanol	−0.68/0.65	−0.68/0.65	−0.73/0.69	−0.82/0.77
acetonitrile	−0.62/0.61	−0.62/0.60	−0.67/0.64	−0.76/0.73
dichloromethane	−0.57/0.56	−0.57/0.55	−0.60/0.59	−0.69/0.67

Table 4. Representative Bond Lengths (in Å) at the Geometries Optimized at the DFT/6-31+G(d,p)/PCMSMD Level with the LC-BOP/B3LYP Functionals

solvent	O−C1	C1−C2	C2−C3	C4−C7	C7−C8
trihydrate crystal[113]	1.304	1.414	1.379	1.441	1.346
water	1.29/1.29	1.43/1.44	1.38/1.38	1.44/1.43	1.36/1.38
methanol	1.29/1.28	1.43/1.44	1.38/1.38	1.44/1.43	1.36/1.38
acetonitrile	1.27/1.27	1.44/1.45	1.37/1.38	1.43/1.42	1.37/1.38
dichloromethane	1.26/1.26	1.45/1.45	1.37/1.37	1.42/1.42	1.37/1.39
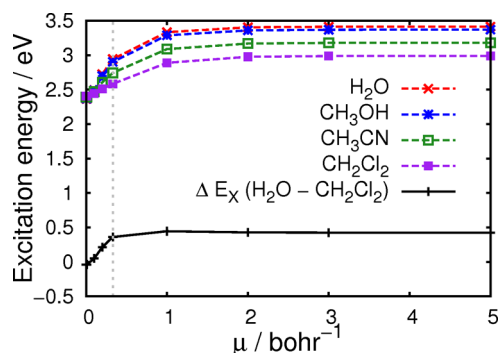
Figure 2. Dependence of the excitation energies and solvatochromic shift from dichloromethane to water (ΔE_X) on the range separation parameter μ in the LC-BOP/PCMSMD calculations. The vertical dotted line is drawn at the default μ value (0.33 bohr^{-1}).

It is worthwhile to mention about the charge transfer character of the excitation of the dye. The previous studies and the present results about the ground and excited states' dipole moments (Table 2) indicate that the S_0-S_1 excitation has some CT character.[19] The CT excitation may be classified as a spatially overlapped one and as a spatially separated one (i.e., the density transfer excitation as discussed in ref 28.). The latter is known to be difficult to correctly treat unless an LC functional is used. In order to know which type the present CT excitation belongs to, the lambda diagnostic test was utilized.[117] It evaluates the overlap λ between the occupied and unoccupied orbitals relevant to the excitation; a small value of λ indicates that the excitation has a spatially separated CT or Rydberg character. The calculated values are among 0.54 and 0.71[118] indicating that the excitation has a spatially overlapped CT character. Thus, this excitation could be correctly modeled even with functionals other than LC ones. Actually, the absolute values of the excitation energy in solutions calculated with the B3LYP functional seems to be on average in good agreement with the experimental values. However, as has already been mentioned above, functionals with no or little HF exchange provide less satisfactory results for the solvatochromic shift than LC functionals because of a delocalization tendency of the former functionals due to the artificial self-interaction error,[40,43]

which results in the poor description of polarization of the merocyanine dye in polar solvents at the ground state with benzenoid character.

Hydrogen Bonding Effects. We have seen above that we can partly reproduce the large solvatochromic shift of Brooker's merocyanine with the PCMSMD method by appropriately choosing a density functional with a large amount of HF exchange. However, the calculated shifts of about 0.4 eV by using an LC functional are still smaller than the experimentally observed shift of 0.76 eV for dichloromethane to water. As previous studies have suggested,[16,19] the remaining discrepancy between the experimental and theoretical results can be the solute−solvent hydrogen bonds which cannot be adequately described by implicit solvation models. Therefore, we next investigate the effects of the explicit description of solute−solvent hydrogen bonds on the solvatochromic shift by using the RISM-SCF-SEDD and MF-QM/MM methods. The excitation energies calculated by these methods with the LC-BOP functional (with the default value of $\mu = 0.33$) are presented in Table 5 together with the PCM with only bulk electrostatic interactions, PCMSMD results, and the experimental values. The geometries in solutions were optimized by the respective solvation models.[119] The RISM-SCF-SEDD and MF-QM/MM calculations produce the solvatochromic shifts from dichloromethane to water by 0.72 and 0.66 eV, both of which are in good agreement with the experimental value (0.76 eV). As we have seen, the PCMSMD also gives reasonable results though the shift (0.36 eV) is only about half of the experimental value. The PCM calculations further underestimate the solvatochromic shift by as much as 0.57 eV. These results clearly show that an explicit description of hydrogen bonds is vital to correctly model the solvatochromism of the dye as shown in the previous study.[12,16,23,19] It is also revealed that it is possible to quantitatively estimate the large solvatochromic shift from TDDFT calculations when we choose an LC functional which recovers 100% HF exchange in the long-range limit even with the default value of μ. Note that though we used here the LC-BOP functional in combination with the explicit solvation models, it is also expected to work well for reproducing the experimental large solvatochromic shift if we use, for example, the M06-HF

Table 5. Excitation Energies and Solvatochromic Shifts (in Parentheses) from Dichloromethane Calculated at the LC-BOP/6-31+G(d,p) Level Combined with the Solvation Models^c

solvent	PCM	PCMSMD	RISM-SCF-SEDD^{a,b}	MF-QM/MM^a	expt
water	2.77(0.19)	2.94(0.36)	3.18(0.72)	3.20(0.66)	2.81(0.76)
methanol	2.74(0.16)	2.90(0.32)	2.82(0.36)	2.91(0.37)	2.57(0.52)
acetonitrile	2.74(0.16)	2.74(0.16)	2.64(0.18)	2.73(0.19)	2.17(0.12)
dichloromethane	2.58(0.00)	2.58(0.00)	2.46(0.00)	2.54(0.00)	2.05(0.00)

^{a}The nonequilibrium solvation effects are included. See the text for details. ^{b}The geometries optimized by using the MF-QM/MM method were used. ^{c}Units are in eV.

functional.[120] It should be emphasized that we also tested the B3LYP functional in the MF-QM/MM calculations and found that the calculated solvatochromic shift from dichloromethane to water was 0.17 eV, which was much smaller than that calculated using the LC-BOP functional (0.66 eV) and the experimental one (0.76 eV). This is probably because of the inadequate description of the polarization (the benzenoid character) of the merocyanine dye at the ground state in polar solvents when the B3LYP functional is used as shown in the previous section. This can make the difference in the solvation effects rather small between the protic and aprotic solvents, and then the solvatochromic shifts are underestimated.

The PCM model was found to produce almost the same excitation energies for all the solvents except for dichloromethane. It can be understood from the following reason; the present PCM calculations take into account only the solute—solvent electrostatic interactions, whose difference between the solvents originates from only the relative dielectric constants. The static (optical) dielectric constants are 78.39 (1.78) for water, 32.63 (1.76) for methanol, 35.69 (1.81) for acetonitrile, and 8.93 (2.02) for dichloromethane, respectively. Since the electrostatic interactions in the dielectric continuum model are rather insensitive to the dielectric constant once the value becomes greater than 30, the results related to the properties in the ground state (geometry and polarization) for the three solvents are expected to be similar. Moreover, since the optical dielectric constants are not so different among all of the solvents, the nonequilibrium solvation effects on the excitation energies are also expected to be similar. They were estimated to be −0.19, −0.19, −0.20, and −0.25 eV for water, methanol, acetonitrile, and dichloromethane, respectively, which confirms the above expectation.

It is interesting to note that, unlike the PCM model, the PCMSMD can describe the differences between the aprotic and protic solvents because of its CDS correction to the solute—solvent interactions. They influence the geometries as can be seen in Table 4 and then the weights of the two resonance forms, resulting in the differences in the excitation energies between the solvents. It is also interesting that the PCMSMD results are very similar to those from the MF-QM/MM calculations not only for aprotic solvents but also for a protic methanol. This indicates that the CDS correction can mimic the solute—solvent hydrogen bonds at least to some extent.

Another important feature to mention is that the explicit solvation models can describe the difference between methanol and water. The calculated solvatochromic shifts from methanol to water are 0.36 and 0.29 eV for the RISM-SCF-SEDD and MF-QM/MM methods, respectively. These values are in reasonable agreement with the corresponding experimental one (0.24 eV). On the other hand, the PCM and PCMSMD calculations severely underestimate the shift to be 0.03 and 0.04 eV. It should be stressed that the overestimation of the excitation energies calculated by using the explicit solvation models is not an error caused by the solvation models but most probably by an inherent problem of the TDDFT calculation with approximate XC functionals. An inadequate treatment of electron correlation in the ground and especially excited states can be a source of the overestimation, which will be addressed later.

In order to further investigate the effects of explicit description of solvent molecules (especially solute—solvent hydrogen bonds) on the increased solvatochromic shift, we first examine the solvation structures of the dye: the radial

distribution functions (RDFs) and the spatial distribution functions (SDFs) in water and methanol shown in Figure 3 and
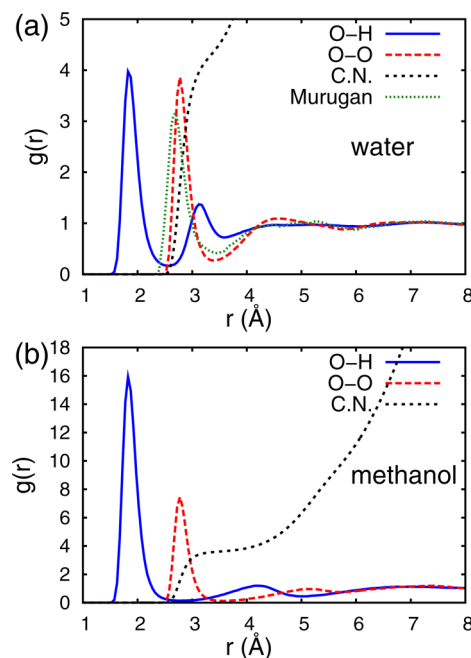

Figure 3. Radial distribution functions and coordination numbers of (a) water and (b) the hydroxyl group of methanol around the phenolate oxygen in the Brooker's merocyanine obtained from the mean-field QM/MM calculations. The green dotted line in (a) is the RDF between the phenolate oxygen of the Brooker's merocyanine and the center of mass of water molecules taken from the result of the CPMD-QM/MM calculations by Murugan et al.[19]

Figure 4, respectively, obtained from the MF-QM/MM calculations. The RDF between the phenolate oxygen and water oxygen is in good agreement with the RDF between the phenolate oxygen and the center of mass of water molecules obtained from the CPMD-QM/MM calculations of Murugan et al.[19] The peak height of our result is slightly higher probably because the solute (Brooker's merocyanine) becomes more polarized due to the use of the LC-BOP functional in our work rather than the BLYP functional used in their work based on the discussion in the previous section and in Table 2 and Table 3. The sharp first peaks in the RDFs indicate the existence of solute—solvent hydrogen bonds in water and methanol, which can be also verified from the SDFs. Although the peak for methanol is significantly higher than that for water, the coordination numbers around the phenolate oxygen are 3.6 and 4.3 for methanol and water, respectively.[121] It suggests that the effects of the hydrogen bonds can be larger in water than in methanol, which are consistent with the excitation energies in these two solvents (Table 5). Interestingly, it can be seen from the SDFs that on the one hand water molecules tend to reside on the phenolate ring, but on the other hand methanol molecules do not. This could also contribute to make differences in the electronic states and the excitation energies of the dye in these two solvents. The SDFs also show that there is little distribution of oxygen of water molecules near the nitrogen atom. This can be understood because the positive charge is delocalized over the pyridyl ring and is not localized on the N−CH$_3$ group as we will see later in Table 7.[19]
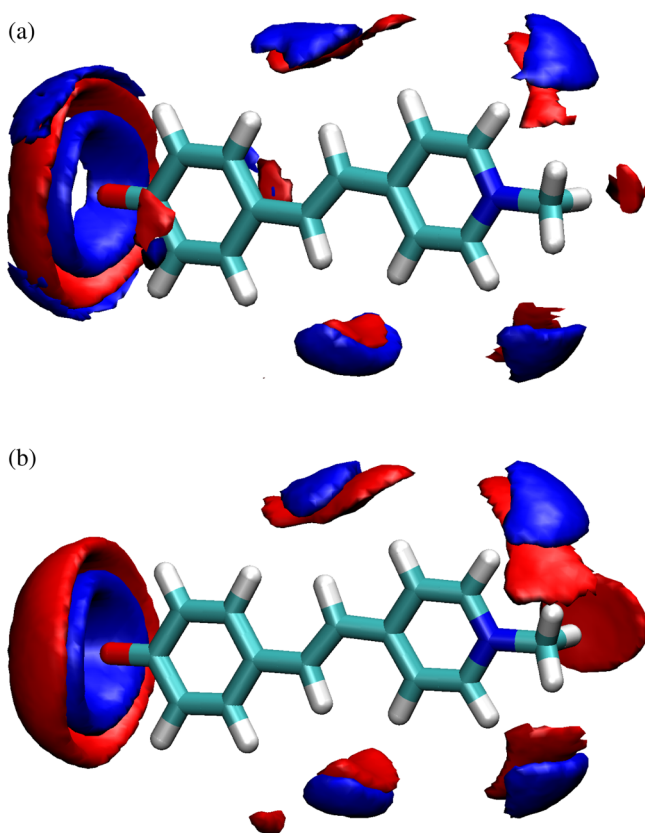
Figure 4. Spatial distribution functions of (a) water and (b) the hydroxyl group of methanol around the Brooker's merocyanine obtained from the mean-field QM/MM calculations. The blue and red isosurfaces (color online) represent the regions where the number densities of the hydrogen atom and the oxygen atom of solvent molecules are five times higher than the bulk values, respectively.

We compare the ground state dipole moment and atomic or fragment charges of the dye in Table 6 and Table 7 calculated

Table 6. Dipole Moments (in Debye) in the Ground State Calculated at the LC-BOP/6-31+G(d,p) Level Combined with the Solvation Models

solvent	PCM	PCMSMD	RISM-SCF-SEDD	MF-QM/MM
water	35.4	38.6	41.8	41.6
methanol	34.8	37.9	36.7	38.2
acetonitrile	34.9	34.6	31.8	33.7
dichloromethane	31.7	31.6	24.1	28.0

by the four solvation models to investigate the effects of the explicit description of solute−solvent interactions on the solute polarization. The general trend that the solute is more polarized in more polar and especially protic solvents can be observed for the PCMSMD and the two explicit solvation models. The PCM model with only the bulk electrostatic interactions cannot adequately distinguish water, methanol, and acetonitrile. As for the excitation energies, the dipole moments and partial charges in acetonitrile and methanol calculated by the PCMSMD and the MF-QM/MM methods are rather similar to each other, although the former is an implicit solvation model and the latter is an explicit one. The solute polarization in water is underestimated by the two implicit solvation models as compared to the explicit models, which is well correlated with the underestimation of the solvatochromic shift by the implicit models. We also observe some difference for dichloromethane between the implicit and explicit solvation models. The results for dichloromethane indicate that the dye is less polarized in the solvent when calculated by the explicit solvation models than by the implicit ones. This may be due to the lack of explicit polarization effects of the solvent in the explicit solvation models using nonpolarizable force fields for the solvent.[60,122] The atomic charge of the phenolate oxygen in protic solvents increases when we use the explicit solvation models, which results from the hydrogen bonds between the phenolate oxygen and the solvent hydrogen and local polarization of the dye. Note that while negative charge about $-0.7|e| \sim -0.9|e|$ is localized on the phenolate oxygen in the phenolate moiety, positive charge residing on the N−CH$_3$ moiety is almost zero in all of the solvents and $0.6|e| \sim 0.9|e|$ charge is delocalized over the methylpyridinium moiety.

We have seen so far that the large solvatochromic shift of the dye can be reproduced from a theoretical calculation when we choose a density functional with a considerable amount of HF exchange (thus an LC functional with 100% HF exchange in long-range limit is recommended) and employ an explicit solvation model like the RISM-SCF-SEDD or MF-QM/MM method. However, overestimations of the excitation energy with respect to the experimental values are observed. We suspect that it comes from an inadequate treatment of electron correlation in the density functionals. In order to verify this, we first performed SAC-CI/PCM calculations[123] with a Gaussian09 program package[124] at the geometries optimized at the LC-BOP/6-31+G(d,p) level. The excitation energies at the SAC-CI/MF-QM/MM level were then estimated as follows (and also the corresponding estimations by using the PCMSMD and RISM-SCF-SEDD)

Table 7. Phenolate/Methylpyridinium (First Line) and Phenolate Oxygen/N−CH$_3$ (Second Line) Fragment Charges in Solutions in the Ground State Calculated from Natural Population Analysis at the LC-BOP/6-31+G(d,p) Level Combined with the Solvation Models

solvent	PCM	PCMSMD	RISM-SCF-SEDD	MF-QM/MM
water	−0.77/0.73	−0.83/0.78	−0.87/0.80	−0.87/0.81
	−0.82/-0.01	−0.88/0.00	−0.94/0.00	−0.93/0.01
methanol	−0.76/0.72	−0.82/0.77	−0.79/0.74	−0.82/0.76
	−0.81/-0.02	−0.87/0.00	−0.85/-0.02	−0.89/-0.01
acetonitrile	−0.76/0.72	−0.76/0.73	−0.71/0.68	−0.75/0.71
	−0.82/-0.02	−0.78/-0.01	−0.75/-0.03	−0.77/-0.02
dichloromethane	−0.69/0.66	−0.69/0.67	−0.55/0.54	−0.65/0.62
	−0.78/-0.04	−0.75/-0.03	−0.69/-0.08	−0.74/-0.05

H

dx.doi.org/10.1021/ct5004884 | J. Chem. Theory Comput. XXXX, XXX, XXX−XXX

Table 8. Excitation Energies and Solvatochromic Shifts (in Parentheses) from Dichloromethane at the SAC-CI/6-31+G(d,p) Levels[b]

solvent	PCM[a]	PCMSMD[a]	RISM-SCF-SEDD[a]	MF-QM/MM[a]	expt
water	2.40(0.38)	2.57(0.55)	2.79(0.87)	2.81(0.81)	2.81(0.76)
methanol	2.32(0.30)	2.48(0.46)	2.33(0.41)	2.42(0.42)	2.57(0.52)
acetonitrile	2.23(0.21)	2.23(0.21)	2.17(0.25)	2.26(0.26)	2.17(0.12)
dichloromethane	2.02(0.00)	2.02(0.00)	1.92(0.00)	2.00(0.00)	2.05(0.00)

[a]The nonequilibrium solvation effects were included. See the main text (eq 3). [b]Units are in eV.

$$\Delta E_{\text{SAC-CI}}^{\text{MF-QM/MM}}(X) \simeq \Delta E_{\text{SAC-CI}}^{\text{PCM}}(X) + (\Delta E_{\text{LC-BOP}}^{\text{MF-QM/MM}}(X) - \Delta E_{\text{LC-BOP}}^{\text{PCM}}(X)) + \Delta\omega_{\text{LC-BOP}}^{\text{noneq}}(X)$$

$$(3)$$

where ΔE stands for the calculated excitation energy, and X denotes a solvent (water, methanol, acetonitrile, dichloromethane). The second term corrects the difference between the solvation model employed and PCM. The third term denotes the nonequilibrium solvation effect described in Computational Details.[125] This approximation works well when the solute electron densities at the LC-BOP, HF, and SAC levels are not so much different from each other. Note that the SAC-CI includes an equivalent of 100% HF exchange, which was shown above to be important for accurately modeling the solvatochromism. Table 8 lists the estimated excitation energies along with the solvatochromic shift from dichloromethane to each solvent, which are in very good agreement with the experimental values when we use the explicit solvation models. These results support our speculation that the overestimation of the excitation energies mainly comes from inadequate treatment of electron correlation effects in the density functionals and not from some defects of the explicit solvation models. In other words, as long as we use an explicit solvation model and an electronic structure method including sufficient electron correlations, it is possible to give quantitative results for both of the excitation energies and the large solvatochromic shift of the Brooker's merocyanine in solutions as expected. There remain, however, some differences between the calculated excitation energies using explicit solvation models and the experimental ones. The discrepancies may come from the classical description of the solvent molecules and solute–solvent interactions in these calculations, which can be improved by using a more elaborate solvent model like a polarizable one[19,60] or a more *ab initio* based model such as effective fragment potential (EFP).[126]

CONCLUDING REMARKS

In this paper, we theoretically investigated the solvatochromism of the Brooker's merocyanine in protic and aprotic solvents by the combined use of TDDFT with mean-field solvation theories. First, the functional dependence of the solvatochromic shift was examined. It reveals that the amount of HF exchange included in the functional is the most important factor to reproduce the solvatochromic shift between the solvents. The LDA, GGA, and meta-GGA functionals without HF exchange give a small bathochromic shift against the experimentally observed large hypsochromic shift. The hybrid functionals with a small amount (≤20%) of HF exchange produce the correct hypsochromic shift, but the value is significantly underestimated compared to that from a calculation with an LC functional which recovers 100% HF exchange in the asymptotic region. Second, the effects of the explicit description of the

solute–solvent interactions were investigated by comparing the PCM and PCMSMD methods and the RISM-SCF-SEDD and MF-QM/MM methods. The hydrogen bonds especially in water are necessary to be explicitly handled to accurately reproduce the solvatochromic shift from dichloromethane to water and also from methanol to water. The PCM which describes only the bulk electrostatic interactions cannot describe the differences between water, methanol, and acetonitrile. The PCMSMD including both the electrostatic and nonelectrostatic interactions can distinguish the three solvents but considerably underestimate the solvatochromic shift from methanol to water. On the other hand, both of the RISM-SCF-SEDD and MF-QM/MM methods quantitatively reproduce the experimental large solvatochromic shift from dichloromethane to water and also give reasonable shifts from methanol to water.

In order to clarify the reason the excitation energies obtained from the LC-TDDFT calculations with explicit solvent models overestimate the experimental values, we also performed the SAC-CI/PCM calculations and extrapolated the values to estimate the excitation energies calculated at the SAC-CI/RISM-SCF-SEDD and MF-QM/MM levels. The estimated values are in excellent agreement with the experimental ones. It indicates that the overestimations by the LC-TDDFT calculations originate from the inadequate treatment of electron correlations in the density functional used.

At first sight, the TDDFT/PCM calculation with the popular B3LYP functional seems to give accurate excitation energy in water. However, it never means that the level of calculation is reliable since it results from a fortunate cancellation of errors: the overestimation due to an inadequate treatment of electron correlations in the density functional and an underestimation because of the absence of the explicit solute–solvent hydrogen bonds in the implicit solvation model. Actually, the level cannot reproduce the large solvatochromic shift from dichloromethane to water. It can be reproduced only when an appropriate functional such as an LC functional with 100% HF exchange in the asymptotic region is employed and the solute–solvent hydrogen bonds are explicitly taken into account by a precise solvation model. The present study will provide a useful guideline for theoretical study on a solvatochromic behavior of a dye molecule in condensed phases when we use the TDDFT to calculate the excitation energy.

ASSOCIATED CONTENT

Ⓢ Supporting Information

The LJ parameters used in the RISM-SCF-SEDD and MF-QM/MM calculations and the excitation energies calculated by varying the number of configurations in the MF-QM/MM calculations. This material is available free of charge via the Internet at http://pubs.acs.org.

■ AUTHOR INFORMATION

Corresponding Authors
*E-mail: hnaka@moleng.kyoto-u.ac.jp.
*E-mail: hirofumi@moleng.kyoto-u.ac.jp.

Notes
The authors declare no competing financial interest.

■ REFERENCES

(1) Reichardt, C. *Solvents and Solvent Effects in Organic Chemistry*, 3rd ed.; VCH-Wiley: Weinheim, Germany, 2003.

(2) Reichardt, C. Solvatochromic Dyes as Solvent Polarity Indicators. *Chem. Rev.* **1994**, *94*, 2319.

(3) Testoni, F. M.; Ribeiro, E. A.; Giusti, L. A.; Machado, V. G. Merocyanine solvatochromic dyes in the study of synergistic effects in mixtures of chloroform with hydrogen-bond accepting solvents. *Spectrochim. Acta, Part A* **2009**, *71*, 1704.

(4) Cavalli, V.; da Silva, D. C.; Machado, C.; Machado, V. G.; Soldi, V. The Fluorosolvatochromism of Brooker's Merocyanine in Pure and in Mixed Solvents. *J. Fluoresc.* **2006**, *16*, 77.

(5) Kashida, H.; Sano, K.; Hara, Y.; Asanuma, H. Modulation of pK_a of Brooker's Merocyanine by DNA Hybridization. *Bioconj. Chem.* **2009**, *20*, 258.

(6) Shiraishi, Y.; Inoue, T.; Hirai, T. Local Viscosity Analysis of Triblock Copolymer Micelle with Cyanine Dyes as a Fluorescent Probe. *Langmuir* **2010**, *26*, 17505.

(7) Bussemer, B.; Dreiling, I.; Grummt, U. W.; Mohr, G. J. Spectroscopic and quantum chemical study of the Brønsted acid sites in zeolite L channels with acidochromic cyanine dyes. *J. Photochem. Photobiol., A* **2009**, *240*, 90.

(8) Venturini, C. G.; Andreaus, J.; Machado, V. G.; Machado, C. Solvent effects in the interaction of methyl-β-cyclodextrin with solvatochromic merocyanine dyes. *Org. Biomol. Chem.* **2005**, *3*, 1751.

(9) Brooker, L. G. S.; Keyes, G. H.; Heseltine, D. W. Color and Constitution. XI. Anhydronium Bases of *p*-Hydroxystyryl Dyes as Solvent Polarity Indicators. *J. Am. Chem. Soc.* **1951**, *73*, 5350.

(10) Würthner, F.; Archetti, G.; Schmidt, R.; Kuball, H. G. Solvent Effect on Color, Band Shape, and Charge-Density Distribution for Merocyanine Dyes Close to the Cyanine Limit. *Angew. Chem., Int. Ed.* **2008**, *47*, 4529.

(11) Steiner, U.; Abdel-Kader, M. H.; Fischer, P.; Kramer, H. E. A. Photochemical Cis/Trans Isomerization of a Stilbazolium Betaine. A Protolytic/Photochemical Reaction Cycle. *J. Am. Chem. Soc.* **1978**, *78*, 3190.

(12) Tsukada, M.; Mineo, Y.; Itoh, K. Resonance Raman and Surface-Enhanced Resonance Raman Scattering Study on Structure of a Merocyanine Dye, 4-(2-(4-Hydroxyphenyl)ethenyl)-1-methylpyridinium. *J. Phys. Chem.* **1989**, *93*, 7989.

(13) Gruda, I.; Bolduc, F. Spectral Properties and Basicity of Stilbazolium Betaines Containing Bulky Substituents on the Quinoid Ring. *J. Org. Chem.* **1984**, *49*, 3300.

(14) Burda, C.; Abdel-Kader, M. H.; Link, S.; El-Sayed, M. A. Femtosecond Dynamics of a Simple Merocyanine Dye: Does Deprotonation Compete with Isomerization? *J. Am. Chem. Soc.* **2006**, *122*, 6720.

(15) Botrel, A.; Le Beuze, A.; Jacques, P.; Strub, H. Solvatochromism of a Typical Merocyanine Dye. *J. Chem. Soc., Faraday Trans. 2* **1984**, *80*, 1235.

(16) Morley, J. O.; Morley, R. M.; Docherty, R.; Charlton, M. H. Fundamental Studies on Brooker's Merocyanine. *J. Am. Chem. Soc.* **1997**, *119*, 10192.

(17) Domínguez, M.; Rezende, M. C. Towards a unified view of the solvatochromism of phenolate betaine dyes. *J. Phys. Org. Chem.* **2010**, *23*, 156.

(18) Adjaye-Mensah, E.; Gonzalez, W. G.; Miksovska, J.; Wilson, J. N. Photophysical Characterization of a Benzo-Fused Analogue of Brooker's Merocyanine: Solvent Polarity and pH Effects. *J. Phys. Chem. A* **2012**, *116*, 12470.

(19) Murugan, N. A.; Kongsted, J.; Rinkevicius, Z.; Aidas, K.; Ågren, H. Modeling the Structure and Absorption Spectra of Stilbazolium Merocyanine in Polar and Nonpolar Solvents Using Hybrid QM/MM Techniques. *J. Phys. Chem. B* **2010**, *114*, 13349.

(20) Baraldi, I.; Brancolini, G.; Momicchioli, F.; Ponterini, G.; Vanossi, D. Solvent influence on absorption and fluorescence spectra of merocyanine dyes: a theoretical and experimental study. *Chem. Phys.* **2003**, *288*, 309.

(21) Mascayano, C.; Rezende, M. C.; Mendez, C.; Núñez, G.; Chiang, V. Solute-Solvent Interactions in Solutions of Solvatochromic Phenoxides: A Dynamics Simulation Study. *J. Solution Chem.* **2009**, *38*, 363.

(22) Abdel-Halim, S. T.; Awad, M. K. Absorption, fluorescence, and semiempirical ASED-MO studies on a typical Brooker's merocyanine dye. *J. Mol. Struct.: THEOCHEM* **2005**, *754*, 16.

(23) Jacques, P. On the Relative Contributions of Nonspecific and Specific Interactions to the Unusual Solvatochromism of a Typical Merocyanine Dye. *J. Phys. Chem.* **1986**, *90*, 5535.

(24) Catalán, J.; Mena, E.; Meutermans, W.; Elguero, J. Solvatochromism of a Typical Merocyanine: Stilbazolium Betaine and Its 2,6-Di-tert-butyl Derivative. *J. Phys. Chem.* **1992**, *96*, 3615.

(25) Luzhkov, V.; Warshel, A. Microscopic Calculations of Solvent Effects on Absorption Spectra of Conjugated Molecules. *J. Am. Chem. Soc.* **1991**, *113*, 4491.

(26) Kovalenko, S. A.; Eilers-König, N.; Senyushkina, T. A.; Ernsting, N. P. Charge Transfer and Solvation of Betaine-30 in Polar Solvents - A Femtosecond Broadband Transient Absorption Study. *J. Phys. Chem. A* **2001**, *105*, 4834.

(27) Neese, F. Prediction of molecular properties and molecular spectroscopy with density functional theory: From fundamental theory to exchange-coupling. *Coord. Chem. Rev.* **2009**, *253*, 526.

(28) Casida, M. E. Time-dependent density-functional theory for molecules and molecular solids. *J. Mol. Struct.: THEOCHEM* **2009**, *914*, 3.

(29) Ullrich, C. A. *Time-Dependent Density-Functional Theory*; Oxford University Press: New York, 2012.

(30) Barone, V.; Improta, R.; Rega, N. Quantum Mechanical Computations and Spectroscopy: From Small Rigid Molecules in the Gas Phase to Large Flexible Molecules in Solution. *Acc. Chem. Res.* **2008**, *41*, 605.

(31) Jacquemin, D.; Perpete, E. A.; Ciofini, I.; Adamo, C. Accurate Simulation of Optical Properties in Dyes. *Acc. Chem. Res.* **2009**, *42*, 326.

(32) van Faassen, M.; Burke, K. Time-dependent density functional theory of high excitations: to infinity, and beyond. *Phys. Chem. Chem. Phys.* **2009**, *11*, 4437.

(33) Besley, N. A.; Asmuruf, F. A. Time-dependent density functional theory calculations of the spectroscopy of core electrons. *Phys. Chem. Chem. Phys.* **2010**, *12*, 12024.

(34) Barone, V.; Polimeno, A. Integrated computational strategies for UV/vis spectra of large molecules in solution. *Chem. Soc. Rev.* **2007**, *36*, 1724.

J

dx.doi.org/10.1021/ct5004884 | *J. Chem. Theory Comput.* XXXX, XXX, XXX−XXX

(35) Pastore, M.; Mosconi, E.; Angelis, F. D.; Grätzel, M. A Computational Investigation of Organic Dyes for Dye-Sensitized Solar Cells: Benchmark, Strategies, and Open Issues. *J. Phys. Chem. C* **2010**, *114*, 7205.

(36) Jacquemin, D.; Mennucci, B.; Adamo, C. Excited-state calculations with TD-DFT: from benchmarks to simulations in complex environments. *Phys. Chem. Chem. Phys.* **2011**, *13*, 16987.

(37) Mennucci, B.; Caricato, M.; Ingrosso, F.; Cappelli, C.; Cammi, R.; Tomasi, J.; Scalmani, G.; Frisch, M. J. How the Environment Controls Absorption and Fluorescence Spectra of PRODAN: A Quantum-Mechanical Study in Homogeneous and Heterogeneous Media. *J. Phys. Chem. B* **2008**, *112*, 414.

(38) Dreuw, A.; Head-Gordon, M. Single-Reference ab Initio Methods for the Calculaion of Excited States of Large Molecules. *Chem. Rev.* **2005**, *105*, 4009.

(39) Dreuw, A.; Head-Gordon, M. Failure of Time-Dependent Density Functional Theory for Long-Range Charge-Transfer Excited States: The Zincbacteriochlorin-Bacteriochlorin and Bacteriochlor-ophyll-Spheroidene Complexes. *J. Am. Chem. Soc.* **2004**, *126*, 4007.

(40) Lundberg, M.; Siegbahn, P. E. M. Quantifying the effects of the self-interaction error in DFT: When do the delocalized states appear? *J. Chem. Phys.* **2005**, *122*, 224103.

(41) Perdew, J. P.; Ruzsinszky, A.; Tao, J.; Staroverov, V. N.; Scuseria, G. E.; Csonka, G. I. Prescription for the design and selection of density functional approximations: More constraint satisfaction with fewer fits. *J. Chem. Phys.* **2005**, *123*, 062201.

(42) Livshits, E.; Baer, R. A well-tempered density functional theory of electrons in molecules. *Phys. Chem. Chem. Phys.* **2007**, *9*, 2932.

(43) Vydrov, O. A.; Scuseria, G. E. Assessment of a long-range corrected hybrid functional. *J. Chem. Phys.* **2006**, *125*, 234109.

(44) Tozer, D. J.; Amos, R. D.; Handy, N. C.; Roos, B. O.; Serrano-Andrés, L. Does density functional theory contribute to the understanding of excited states of unsaturated organic compounds? *Mol. Phys.* **1999**, *97*, 859.

(45) Baer, R.; Livshits, E.; Salzner, U. Tuned Range-Separated Hybrids in Density Functional Theory. *Annu. Rev. Phys. Chem.* **2010**, *61*, 85.

(46) Kityk, A. V. Absorption and Fluorescence Spectra of Heterocyclic Isomers from Long-Range-Corrected Density Functional Theory in Polarizable Continuum Approach. *J. Phys. Chem. A* **2012**, *116*, 3048.

(47) *Continuum Solvation Models in Chemical Physics*; Mennucci, B., Cammi, R., Eds.; John Wiley & Sons: Chichester, 2007.

(48) Tomasi, J.; Mennucci, B.; Cammi, R. Quantum Mechanical Continuum Solvation Models. *Chem. Rev.* **2005**, *105*, 2999.

(49) Marenich, A. V.; Cramer, C. J.; Truhlar, D. G. Universal Solvation Model Based on Solute Electron Density and on a Continuum Model of the Solvent Defined by the Bulk Dielectric Constant and Atomic Surface Tensions. *J. Phys. Chem. B* **2009**, *113*, 6378.

(50) Mennucci, B.; Cappelli, C.; Guido, C. A.; Cammi, R.; Tomasi, J. Structures and Properties of Eelectronically Excited Chromophores in Solution from the Polarizable Continuum Model Coupled to the Time-Dependent Density Functional Theory. *J. Phys. Chem. A* **2009**, *113*, 3009.

(51) Tomasi, J. Thirty years of continuum solvation chemisty: a review, and prospects for the near future. *Theor. Chem. Acc.* **2004**, *112*, 184.

(52) Sato, H. A modern solvation theory: quantum chemistry and statistical chemistry. *Phys. Chem. Chem. Phys.* **2013**, *15*, 7450.

(53) *Molecular Theory of Solvation*; Hirata, F., Ed.; Kluwer: New York, 2004.

(54) Ten-no, S.; Hirata, F.; Kato, S. Reference interaction site model self-consistent field study for solvation effect on carbonyl compounds in aqueous solution. *J. Chem. Phys.* **1994**, *100*, 7443.

(55) Sato, H.; Hirata, F.; Kato, S. Analytical energy gradient for the reference interaction site model multiconfigurational self-consistent-field method: Application to 1,2-difluoroethylene in aqueous solution. *J. Chem. Phys.* **1996**, *105*, 1546.

(56) Sato, H.; Kovalenko, A.; Hirata, F. Self-consistent field, ab initio molecular orbital and three-dimensional reference interaction site model study for solvation effect on carbon monoxide in aqueous solution. *J. Chem. Phys.* **2000**, *112*, 9463.

(57) Yokogawa, D.; Sato, H.; Sakaki, S. New generation of the reference interaction site model self-consistent field method: Introduction of spatial electron density distribution to the solvation theory. *J. Chem. Phys.* **2007**, *126*, 244504.

(58) Yokogawa, D.; Sato, H.; Sakaki, S. Analytical energy gradient for reference interaction site model self-consistent field explicitly including spatial electron density distribution. *J. Chem. Phys.* **2009**, *131*, 214504.

(59) Yamamoto, T. Variational and perturbative formulations of quantum mechanical/molecular mechanical free energy with mean-field embedding and its analytical gradients. *J. Chem. Phys.* **2008**, *129*, 244104.

(60) Nakano, H.; Yamamoto, T. Variational calculation of quantum mechanical/molecular mechanical free energy with electronic polar-ization of solvent. *J. Chem. Phys.* **2012**, *136*, 134107.

(61) Nakano, H.; Yamamoto, T. Accurate and Efficient Treatment of Continuous Solute Charge Density in the Mean-Field QM/MM Free Energy Calculation. *J. Chem. Theory Comput.* **2013**, *9*, 188.

(62) Warshel, A.; Levitt, M. Theoretical Studies of Enzymic Reactions: Dielectric, Electrostatic and Steric Stabilization of the Carbonium Ion in the Reaction of Lysozyme. *J. Mol. Biol.* **1976**, *103*, 227.

(63) Field, M. J.; Bash, P. A.; Karplus, M. A combined quantum mechanical and molecular mechanical potential for molecular dynamics simulations. *J. Comput. Chem.* **1990**, *6*, 700.

(64) Warshel, A. *Computer Modeling of Chemical Reactions in Enzymes and Solutions*; Wiley: New York, 2008.

(65) Klähn, M.; Braun-Sand, S.; Rosta, E.; Warshel, A. On Possible Pitfalls in ab Initio Quantum Mechanics/Molecular Mechanics Minimization Approaches for Studies of Enzymatic Reactions. *J. Phys. Chem. B* **2005**, *109*, 15645.

(66) Nakatsuji, H. Cluster expansion of the wavefunction. Excited States. *Chem. Phys. Lett.* **1978**, *59*, 362.

(67) Nakatsuji, H.; Ehara, M. Symmetry adapted cluster-config-uration interaction study on the excited and ionized states of $TiBr_4$ and TiI_4. *J. Chem. Phys.* **1994**, *101*, 7658.

(68) Cossi, M.; Barone, V. Solvent effect on vertical electronic transitions by the polarizable continuum model. *J. Chem. Phys.* **2000**, *122*, 2427.

(69) Cammi, R.; Corni, S.; Mennucci, B.; Tomasi, J. Electronic excitation energies of molecules in solution: State specific and linear response methods for nonequilibrium continuum solvation models. *J. Chem. Phys.* **2005**, *122*, 104513.

(70) Cappelli, C.; Corni, S.; Cammi, R.; Mennucci, B.; Tomasi, J. Nonequilibrium formulation of infrared freqencies and intensities in solution: Analytical evaluation within the polarizable continuum model. *J. Chem. Phys.* **2000**, *113*, 11270.

(71) Tanaka, Y.; Yoshida, N.; Nakano, H. Solvent effect on excited states of merocyanines: A theoretical study using the RISM-SCF method. *Chem. Phys. Lett.* **2013**, *583*, 69.

(72) Nam, K.; Gao, J.; York, D. M. An Efficient Linear-Scaling Ewald Method for Long-Range Electrostatic Interactions in Combined QM/MM Calculations. *J. Chem. Theory Comput.* **2005**, *1*, 2.

(73) *Solvation Effects on Molecules and Biomolecules, Computational Methods and Applications*; Canuto, S., Ed.; Springer: 2008.

(74) Galván, I. F.; Sánchez, M. L.; Martín, M. E.; Olivares del Valle, F. J.; Aguilar, M. A. ASEP/MD: A program for the calculation of solvent effects combining QM/MM methods and the mean field approximation. *Comput. Phys. Commun.* **2003**, *115*, 244.

(75) Galván, I. F.; Sánchez, M. L.; Martín, M. E.; Olivares del Valle, F. J.; Aguilar, M. A. Geometry optimization of molecules in solution: Joint use of the mean field approximation and the free-energy gradient method. *J. Chem. Phys.* **2003**, *118*, 255.

(76) Muñoz-Losa, A.; Galván, I. F.; Aguilar, M. A.; Martín, M. E. Simultaneous Solvent and Counterion Effects on the Absorption

Properties of a Model of the Rhodopsin Chromophore. *J. Chem. Theory Comput.* **2013**, *9*, 1548.

(77) Rosta, E.; Haranczyk, M.; Chu, Z. T.; Warshel, A. Accelerating QM/MM Free Energy Calculations: Representing the Surroundings by an Updated Mean Charge Distribution. *J. Phys. Chem. B* **2008**, *112*, 5680.

(78) Oliveira, L. B. A.; Fonseca, T. L.; Coutinho, K.; Canuto, S. A sequential MC/TD-DFT study of the solvatochromic shift of the pyridinium-*N*-phenoxide betaine dye in water using standard and long-range corrected functionals. *Chem. Phys. Lett.* **2011**, *514*, 251.

(79) Yanai, T.; Tew, D. P.; Handy, N. C. A new hybrid exchange-correlation functional using the Coulomb-attenuating method (CAM-B3LYP). *Chem. Phys. Lett.* **2004**, *21*, 51.

(80) Peach, M. J. G.; Helgaker, T.; Salek, P.; Keal, T. W.; Lutnæs, O. B.; Tozer, D. J.; Handy, N. C. Assessment of a Coulomb-attenuated exchange-correlation energy functional. *Phys. Chem. Chem. Phys.* **2006**, *8*, 588.

(81) Slater, J. C. A Simplification of the Hartree-Fock Method. *Phys. Rev.* **1951**, *81*, 385.

(82) Vosko, S. H.; Wilk, L.; Nusair, M. Accurate spin-dependent electron liquid correlation energies for local spin density calculations: a critical analysis. *Can. J. Phys.* **1980**, *58*, 1200.

(83) Becke, A. D. Density-functional exchange-energy approximation with correct asymptotic behavior. *Phys. Rev. A* **1988**, *38*, 3098.

(84) Lee, C.; Yang, W.; Parr, R. G. Development of the Colle-Salvetti correlation-energy formula into a functional of the electron density. *Phys. Rev. B* **1988**, *37*, 785.

(85) Perdew, J. P.; Burke, K.; Ernzerhof, M. Generalized Gradient Approximation Made Simple. *Phys. Rev. Lett.* **1996**, *77*, 3865.

(86) Perdew, J. P. Density-functional approximation for the correlation energy of the inhomogeneous electron gas. *Phys. Rev. B* **1986**, *33*, 8822.

(87) Tsuneda, T.; Hirao, K. A new spin-polarized Colle-Salvetti-type correlation energy functional. *Chem. Phys. Lett.* **1997**, *268*, 510.

(88) Tsuneda, T.; Suzumura, T.; Hirao, K. A new one-parameter progressive Colle-Salvetti-type correlation functional. *J. Chem. Phys.* **1999**, *110*, 100664.

(89) Perdew, J. P.; Tao, J.; Staroverov, V. N.; Scuseria, G. E. Climbing the Density Functional Ladder: Nonempirical Meta-Generalized Gradient Approximation Designed for Molecules and Solids. *Phys. Rev. Lett.* **2003**, *91*, 146401.

(90) Perdew, J. P.; Tao, J.; Staroverov, V. N.; Scuseria, G. E. Meta-generalized gradient approximation: Explanation of a realistic non-empirical density functional. *J. Chem. Phys.* **2004**, *120*, 6898.

(91) Staroverov, V. N.; Scuseria, G. E.; Tao, J.; Perdew, J. P. Comparative assessment of a new nonempirical density functional: Molecules and hydrogen-bonded complexes. *J. Chem. Phys.* **2003**, *119*, 12129.

(92) Becke, A. D. Density-functional thermochemistry. III. The role of exact exchange. *J. Chem. Phys.* **1993**, *98*, 5648.

(93) Stephens, P. J.; Devlin, F. J.; Chabalowski, C. F.; Frisch, M. J. Ab Initio Calculation of Vibrational Absorption and Circular Dichroism Spectra Using Density Functional Force Fields. *J. Phys. Chem.* **1994**, *98*, 11623.

(94) Hertwig, R. H.; Koch, W. On the parametrization of the local correlation functional. What is Becke-3-LYP? *Chem. Phys. Lett.* **1997**, *268*, 345.

(95) Adamo, C.; Barone, V. Toward reliable density functional methods without adjustable parameters: The PBE0 model. *J. Chem. Phys.* **1999**, *110*, 6158.

(96) Zhao, Y.; Truhlar, D. G. The M06 suite of density functionals for main group thermochemistry, thermochemical kinetics, non-covalent interactions, excited states, and transition elements: two new functionals and systematic testing of four M06-class functionals and 12 other functionals. *Theor. Chem. Acc.* **2008**, *120*, 215.

(97) Zhao, Y.; Truhlar, D. G. Density Functional for Spectroscopy: No Long-Range Self-interaction Error, Good Performance for Rydberg and Charge-Transfer States, and Better Performance on Average than B3LYP for Ground States. *J. Phys. Chem. A* **2006**, *110*, 13126.

(98) Iikura, H.; Tsuneda, T.; Yanai, T.; Hirao, K. A long-range correction scheme for generalized-gradient-approximation exchange functionals. *J. Chem. Phys.* **2001**, *115*, 3540.

(99) Tawada, Y.; Tsuneda, T.; Yanagisawa, S.; Yanai, Y.; Hirao, K. A long-range-corrected time-dependent density functional theory. *J. Chem. Phys.* **2004**, *120*, 8425.

(100) Jacquemin, D.; Perpete, E. A.; Scuseria, G. E.; Ciofini, I.; Adamo, C. TD-DFT Performance for the Visible Absorption Spectra of Organic Dyes: Conventional versus Long-Range Hybrids. *J. Chem. Theory Comput.* **2008**, *4*, 123.

(101) Quinet, O.; Champagne, B. Time-dependent Hartree-Fock schemes for analytical evaluation of the Raman intensities. *J. Chem. Phys.* **2001**, *115*, 6293.

(102) Cornell, W. D.; Cieplak, P.; Bayly, C. I.; Gould, I. R.; Merz, K. M.; Ferguson, D. M.; Spellmeyer, D. C.; Fox, T.; Caldwell, J. W.; Kollman, P. A. A Second Generation Force Field for the Simulation of Proteins, Nucleic Acids, and Organic Molecules. *J. Am. Chem. Soc.* **1995**, *117*, 5179.

(103) Jorgensen, W. L.; Briggs, J. M. Monte Carlo simulations of liquid acetonitrile with a three-site model. *Mol. Phys.* **1988**, *63*, 547.

(104) Jorgensen, W. L.; Madura, J. D.; Swenson, C. J. Optimized intermolecular potential functions for liquid hydrocarbons. *J. Am. Chem. Soc.* **1984**, *106*, 6638.

(105) Jorgensen, W. L. Optimized intermolecular potential functions for liquid alcohols. *J. Phys. Chem.* **1986**, *90*, 1276.

(106) Fox, T.; Kollman, P. A. Application of the RESP Methodology in the Parametrization of Organic Solvents. *J. Phys. Chem. B* **1998**, *102*, 8070.

(107) Schmidt, M. W.; Baldridge, K. K.; Boatz, J. A.; Elbert, S. T.; Gordon, M. S.; Jensen, J. H.; Koseki, S.; Matsunaga, N.; Nguyen, K. A.; Su, S.; Windus, T. L.; Dupuis, M.; Montgomery, J. A. General Atomic and Molecular Electronic Structure System. *J. Comput. Chem.* **1993**, *14*, 1347.

(108) Smith, W.; Forester, T. R.; Todorov, I. T. *DLPOLY 2.20 User Manual*; CCLRC, Daresbury Laboratory: Daresbury, Warrington, 2009.

(109) We take here the S_0-S_2 excitation energy since the excitation has the same character (HOMO−LUMO excitation) as the S_0-S_1 excitation obtained by using hybrid and LC functionals. Moreover, the LDA, GGA, and meta-GGA functionals give almost zero S_0-S_1 oscillator strength.

(110) The range separation parameter in all of the LC functionals used in this study is equal to 0.33 bohr^{-1}.

(111) Foster, J. P.; Weinhold, F. Natural Hybrid Orbitals. *J. Am. Chem. Soc.* **1980**, *102*, 7211.

(112) Reed, A. E.; Weinstock, R. B.; Weinhold, F. Natural population analysis. *J. Chem. Phys.* **1985**, *83*, 735.

(113) De Ridder, D. J. A.; Heijdenrijk, D.; Schenk, H. Structure of 4-{2-[1-Methyl-4(1*H*) -pyridylidene]ethylidene}cyclohexa-2,5-dien-1-one trihydrate. *Acta Crystallogr., Sect. C Cryst. Struct. Commun.* **1990**, *46*, 2197.

(114) Wong, B. M.; Cordaro, J. G. Coumarin dyes for dye-sensitized solar cells: A long-range-corrected density functional study. *J. Chem. Phys.* **2008**, *129*, 214703.

(115) Chiba, M.; Tsuneda, T.; Hirao, K. Excited state geometry optimizations by analytical energy gradient of long-range corrected time-dependent density functional theory. *J. Chem. Phys.* **2006**, *124*, 144106.

(116) It is a possible choice to use different μ for different solvents. However, we did not perform such calculations since it is difficult to prepare any criterion to determine respectively an appropriate value for each solvent.

(117) Peach, M. J. G.; Benfield, P.; Helgaker, T.; Tozer, D. J. Excitation energies in density functional theory: An evaluation and a diagnostic test. *J. Chem. Phys.* **2008**, *128*, 044118.

(118) The smallest and largest values are obtained at the M06-HF in water and SVWN in dichloromethane, respectively, which correlate with the extent of the delocalization of charges in the ground state.

L

dx.doi.org/10.1021/ct5004884 | *J. Chem. Theory Comput.* XXXX, XXX, XXX–XXX

(119) In the RISM-SCF-SEDD calculations, the geometries optimized by the MF-QM/MM method were used.

(120) In fact, the solvatochromic shifts from dichloromethane to water were almost the same (about 0.5 eV) when we compared the results from the M06-HF/PCMSMD and SAC-CI/PCMSMD calculations. It implies that using the M06-HF functional in combination with the explicit solvation models can also reproduce the experimental solvatochromic shifts as the SAC-CI/RISM-SCF-SEDD and SAC-CI/MF-QM/MM calculations as shown in Table 8.

(121) The coordination numbers were calculated as $N(r) = \rho \int_0^r 4\pi r^2 g(r) dr$ where ρ is the number density of a solvent atom. Since the number density of the hydrogen atom of water solvent (about 0.0666 Å^{-3}) is more than four times larger than that of the hydroxyl hydrogen atom of methanol solvent (about 0.0148 Å^{-3}), the first peak of the hydroxyl hydrogen atom of methanol should be about four times higher than that of the hydrogen atom of water to give similar coordination numbers (3.6 and 4.3 for methanol and water, respectively). Similarly, it can also be understood that the peak of the hydroxyl hydrogen atom should be more than two times higher than that of the oxygen atom in methanol solution to give the same coordination number. This is because in addition to the number densities of the atoms are the same, there is an r^2 factor in the integrand of the equation and the peak positions are 2.8 and 1.8 Å for hydroxyl oxygen and hydrogen atoms, respectively.

(122) Acevedo, O.; Jorgensen, W. L. Exploring Solvent Effects upon the Menshutkin Reaction Using a Polarizable Force Field. *J. Phys. Chem. B* **2010**, *114*, 8425.

(123) The SAC-CI calculation was performed using molecular orbitals obtained from the HF/PCM calculation. The nonequilibrium solvation effect was not included in the calculation and then had to be separately taken into account.

(124) Frisch, M. J.; Trucks, G. W.; Schlegel, H. B.; Scuseria, G. E.; Robb, M. A.; Cheeseman, J. R.; Scalmani, G.; Barone, V.; Mennucci, B.; Petersson, G. A.; Nakatsuji, H.; Caricato, M.; Li, X.; Hratchian, H. P.; Izmaylov, A. F.; Bloino, J.; Zheng, G.; Sonnenberg, J. L.; Hada, M.; Ehara, M.; Toyota, K.; Fukuda, R.; Hasegawa, J.; Ishida, M.; Nakajima, T.; Honda, Y.; Kitao, O.; Nakai, H.; Vreven, T.; Montgomery, J. A., Jr.; Peralta, J. E.; Ogliaro, F.; Bearpark, M.; Heyd, J. J.; Brothers, E.; Kudin, K. N.; Staroverov, V. N.; Keith, T.; Kobayashi, R.; Normand, J.; Raghavachari, K.; Rendell, A.; Burant, J. C.; Iyengar, S. S.; Tomasi, J.; Cossi, M.; Rega, N.; Millam, J. M.; Klene, M.; Knox, J. E.; Cross, J. B.; Bakken, V.; Adamo, C.; Jaramillo, J.; Gomperts, R.; Stratmann, R. E.; Yazyev, O.; Austin, A. J.; Cammi, R.; Pomelli, C.; Ochterski, J. W.; Martin, R. L.; Morokuma, K.; Zakrzewski, V. G.; Voth, G. A.; Salvador, P.; Dannenberg, J. J.; Dapprich, S.; Daniels, A. D.; Farkas, O.; Foresman, J. B.; Ortiz, J. V.; Cioslowski, J.; Fox, D. J. *Gaussian 09*, Revision B.01; Gaussian, Inc.: Wallingford, CT, 2010.

(125) The nonequilibrium solvation effect was not included in the first term in eq 3 in the present SAC-CI/PCM calculation. Since the effect is included in both of the terms in the second term in eq 3 and then canceled, the third term in eq 3 is necessary.

(126) Gordon, M. S.; Slipchenko, L. V.; Li, H.; Jensen, J. H. The Effective Fragment Potential: a general method for predicting intermolecular interactions. *Annu. Rep. Comput. Chem.* **2007**, *3*, 177.